scientific reports

Check for updates

OPEN

Characterization of circRNA expression profiles and functional roles in a mouse model of liver injury induced by OSA

Qingshi Chen[1,4]✉, Huiting Lai[2,4], Yuwei Chen[3,4], Zhuli Peng[2], Siying Wu[2] & Dexin Liu[2]✉

Despite mounting evidence linking circular RNAs (circRNAs) to various diseases, their specific role in liver damage triggered by obstructive sleep apnea (OSA) remains ambiguous. This study investigates alterations in circRNA expression patterns in a mouse model subjected to chronic intermittent hypoxia (CIH), aiming to elucidate the pathways that lead to liver damage associated with OSA. We established the CIH model and conducted circRNA microarray analysis on liver samples from both CIH and control groups. The findings were substantiated via qRT-PCR. Furthermore, a comprehensive circRNA-miRNA-mRNA (ceRNA) network was developed, followed by the analysis of GO and KEGG pathways to further elucidate the underlying biological processes. We identified 259 differentially expressed circRNAs, comprising 86 that were upregulated and 173 that were downregulated in CIH mice. The ceRNA analysis suggested that these circRNAs may modulate gene expression by sequestering miRNAs. Our findings highlight potential therapeutic targets for liver pathologies associated with OSA.

Keywords Obstructive sleep apnea, circRNAs, Liver injury, Microarray, The NOD-like receptor pathway

In individuals with obstructive sleep apnea (OSA), the upper airway repeatedly narrows or closes off during sleep, which results in reduced blood oxygen levels and fragmented sleep, ultimately resulting in chronic intermittent hypoxia (CIH)[1]. Research has confirmed that OSA is associated with neurocognitive and cardiovascular complications[2,3]. It also contributes to adverse cardiovascular outcomes, such as hypertension[4], myocardial infarction[5], and heart failure[6]. Previous studies have shown that OSA may cause liver damage through multiple mechanisms, including excessive activation of the sympathetic nervous system, oxidative stress responses, abnormal lipid levels, and insulin resistance. These complex factors collectively exert harmful effects on the liver[7,8]. However, research on the underlying mechanisms of OSA-induced liver injury remains quite limited, and its molecular mechanisms are still unclear.

Circular RNA (circRNA), a subclass of non-coding RNA, is distinguished by its covalently closed loop, offering advantages such as stability, conservation, and tissue-specific expression[9]. Currently, advancements in high-throughput RNA sequencing technology have revealed increasing evidence that circRNA plays a significant role in various diseases, including diabetes, neurological disorders, cardiovascular diseases[10] and cancer[11]. Studies suggest that circRNAs regulate miRNA by acting as sponges, inhibiting the miRNA's ability to target mRNA[12]. Additionally, earlier research indicates a link between circRNA and multiple hepatic conditions, containing non-alcoholic fatty liver disease related to metabolic dysfunction, cirrhosis[13], and liver cancer[14]. However, the expression profiles and mechanisms of circRNAs in liver damage associated with OSA remain unclear.

In this study, differentially expressed circular RNAs (DECs) were evaluated to outline their expression patterns in APOE mice with hepatic damage triggered by OSA. We validated eight candidate circRNAs using qRT-PCR. Furthermore, a circRNA-miRNA-mRNA network was established to uncover the important roles of three chosen DECs in CIH-induced liver damage. Finally, the biological roles of the dysregulated circRNAs were assessed through bioinformatics analysis. Based on these studies, we aim to offer new insights into the progression of OSA-related liver injury, which may aid in clinical treatment for this condition.

[1]Department of Endocrinology and Metabolism, The Second Affiliated Hospital of Fujian Medical University, Quanzhou, China. [2]Department of Interventional Therapy, The Second Affiliated Hospital of Fujian Medical University, Quanzhou, China. [3]Department of Cardiology, The Second Affiliated Hospital of Fujian Medical University, Quanzhou, China. [4]These authors contributed equally: Qingshi Chen, Huiting Lai and Yuwei Chen. ✉email: chenqingshi1986@126.com; 22339922@163.com

Materials and methods

Animals

All methods are reported in accordance with ARRIVE guidelines. In this study, we used male APOE mice purchased from Guangdong Yaokang Biotechnology Co., Ltd. This study followed the Guidelines for Care and Use of Laboratory Animals, as outlined by the Federation of European Laboratory Animal Science Associations and was approved by the Animal Care and Use Committee of 2nd Affiliated Hospital of Fujian Medical University (No. 2021-FMU-346).

CIH mouse model

The APOE mice were divided into two groups: a control group and a CIH group. Briefly, the mice designated for the CIH group were placed in a custom chamber fitted with oxygen sensors to assess the O_2 levels. A gas control system connected to the chamber managed the injection of pure nitrogen, reducing the O_2 concentration to 6% for 60 s. Afterward, the system facilitated rapid replacement of O_2, leading to quick reoxygenation, and after another 60 s, the O_2 concentration rose to 21%. The CIH cycle lasting 2 min was repeated 30 times hourly, accumulating to 8 h of each day, totaling 8 weeks. After 8 weeks of CIH exposure, liver tissues were collected following cervical dislocation euthanasia performed by a trained professional under isoflurane anesthesia.

CircRNA microarray analysis

We completed the analysis of the mouse circRNA Array V2 for six samples. The total RNA from all samples were measured using the NanoDrop ND-1000. Arraystar's standard protocol was followed for sample preparation and gene chip hybridization. In brief, Rnase R (Epicentre, Inc.) was applied to degrade the total RNA, eliminating linear RNA and enriching CircRNAs. Subsequently, fluorescent cRNA was generated by amplifying and transcribing the enriched circRNAs using a random primer method. Arraystar Mouse circRNA Array V2 was hybridized with the labeled cRNAs, which were subsequently incubated at 65 °C for 17 h. Following the washing of the slides, we scanned the array using the Agilent Scanner G2505C. The resulting array images were analyzed using Agilent Feature Extraction Software. Additionally, we applied the limma package in R for quantile normalization and a series of data processing. Finally, venn diagram, volcano plot filtering, fold change filtering, heatmap and hierarchical clustering were applied to pinpoint statistically significant DECs between the two groups, recognize the DECs, and visualize the unique circRNA expression patterns between the groups.

qRT-PCR

Based on fold changes, statistical significance, and KEGG pathway analysis, we evaluated the involvement of circRNAs in key pathways related to CIH-induced liver injury, with the pathway enrichment p-value calculated using three methods (EASE-score, Fisher-Pvalue, and Hypergeometric-Pvalue), ultimately selecting eight circRNAs. Subsequently, to validate the microarray results, we performed qRT-PCR analysis. In brief, total RNA extracted from liver tissue samples using TRI Reagent (Sigma, T9424) was converted into complementary DNA (cDNA) using the SuperScript™ III Reverse Transcriptase Kit (Invitroge: 18080-044). For the qRT-PCR process, the 2 × PCR Master Mix and QuantStudio5 Real-time PCR System (Applied Biosystems, USA) were used, adhering to the manufacturer's specifications. The sequences of the PCR primers are shown in Table 1. CircRNAs' relative expression levels, normalized to β-actin, were analyzed through the application of the $2^{-\Delta\Delta CT}$ method.

	Forward and reverse primer	Tm (°C)	Amplicon length (bp)
β-actin	F:5′GTACCACCATGTACCCAGGC3′	60	247
	R:5′AACGCAGCTCAGTAACAGTCC3		
mmu_circRNA_37101	F:5′CGCCACCATTATTGAAAACT3′	60	190
	R:5′CGACCTTAAAGGACCTGCTG3′		
mmu_circRNA_36790	F:5′GGTCATACTGGGTTCACTTGGT3′	60	221
	R:5′CCAGAGGATTTTGAAGTCAGAGT3′		
mmu_circRNA_36551	F:5′GATTACAGCAACTGGACATATTAGG3′	60	173
	R:5′CCTGAGGTGGGAGTTTATCG3′		
mmu_circRNA_35781	F:5′CTGTGCGAGTCTGTGAAAGG3′	60	78
	R:5′AGCAGGATGACGGTGGATAA3′		
mmu_circRNA_38959	F:5′TTCTCTGCTCTGACAGTTGATG3′	60	152
	R:5′TGAGGTGCTTTCTGGGTGTA3′		
mmu_circRNA_44178	F:5′CAAGACCGTGTTCCAGAAAG3′	60	73
	R:5′GATGACATTGCCCATGTAGACT3′		
mmu_circRNA_38398	F:5′TTGATGTGTTCATTCCAGTACGA3′	60	118
	R:5′AGAATAGGCTGGCTGAGAAAG3′		
mmu_circRNA_25178	F:5′CTTGGAAGGAGAACGAAATCA3′	602	191
	R:5′TCGCCACAGAAACAAGACCA3′		

Table 1. Primer sequences used for qRT-PCR.

Establishment of the circRNA/miRNA interaction network

Based on TargetScan and miRanda, we utilized Arraystar's custom miRNA prediction software to identify the interaction targets of circRNA/miRNA. Using seed match sequences, we further constructed the circRNA-miRNA network with Cytoscape 3.6.1. Detailed annotation of all DECs was performed using circRNA/miRNA interaction data.

Creation of a competing endogenous RNA (ceRNA) regulatory network

Following the ceRNA hypothesis, potential miRNAs targets were identified using a tool developed from TargetScan and miRanda. The ceRNA network was established by combining the miRNAs that are commonly targeted.

GO and KEGG pathway analysis

For the purpose of functionally annotating the parent genes of the dysregulated circRNAs, our study further performed GO analysis, encompassing cellular components (CC), molecular functions (MF), and biological processes (BP). We used enrichment scores for the enriched GO terms. Additionally, KEGG pathway analysis helped clarify the signaling networks associated with circRNAs in liver injury caused by OSA[15–17]. The KEGG method identified variations in biological pathways for downstream mRNAs. A threshold of < 0.05 for the p-value was determined.

Statistical analysis

The Student's t-test were applied to analyze all data for comparing circRNA expression levels between the two groups. All results presented in this research were derived from at least three separate experiments and are expressed as the mean ± standard deviation. A significance level of < 0.05 for the p-value was established as statistically significant.

Result

Exposure to CIH caused liver tissue injury

As illustrated in Fig. 1A, the liver tissue of the control group exhibited normal architecture. In contrast, the CIH group showed signs of liver damage, including mild hepatocyte edema, an increased presence of lipid droplet-like vacuoles in the cytoplasm, and fibrin-like eosinophilic exudates in some central veins. Additionally, red blood cells were observed filling both the central veins and interlobular bile ducts (Fig. 1B).

Alterations in the circRNA expression patterns

Through microarray analysis, we identified 259 DECs in liver tissue from both the CIH and normal liver tissue. As shown in the Venn diagram (S1 Fig), 86 circRNAs were upregulated, whereas 173 circRNAs were downregulated. The distribution of all identified dysregulated circRNAs was similar between the two groups (Fig. 2A). The volcano plots and scatter plots effectively visualized the expression differences between the CIH and control groups (Fig. 2B,C). The scatter plot analysis revealed that the majority of circRNAs exhibited less than 1.5-fold variation between the CIH and control groups (black dots). However, a subset of circRNAs showed significant differential expression, with 86 upregulated (highlighted in red) and 173 downregulated (highlighted in green) in CIH-induced liver injury. Hierarchical clustering and heatmap revealed distinct expression patterns of circRNAs across the samples (Fig. 2D and S2 Fig). Figure 3 illustrates the chromosomal distribution and classification of DECs in the CIH group. Upon visualizing the dysregulated circRNAs in a cluster diagram, we observed a widespread distribution across nearly all mouse chromosomes, with chromosome 2 exhibiting the highest concentration (Fig. 3A). In terms of the upregulated circRNAs, 59 are comprised of exons, 16 are

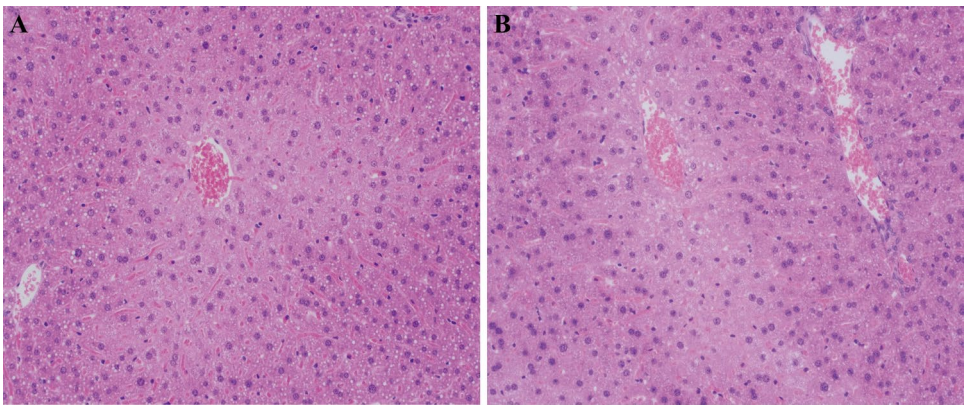

Fig. 1. Histopathological changes in liver tissue. (**A**) Liver histology of the control group mice. (**B**) In the CIH group, which exhibited structural liver abnormalities, mild hepatocyte edema was observed near the central vein, accompanied by an increase in cytoplasmic lipid vacuoles. Additionally, fibrin-like eosinophilic exudates were found in some central veins, and red blood cells filled both the central veins and the interlobular bile ducts.

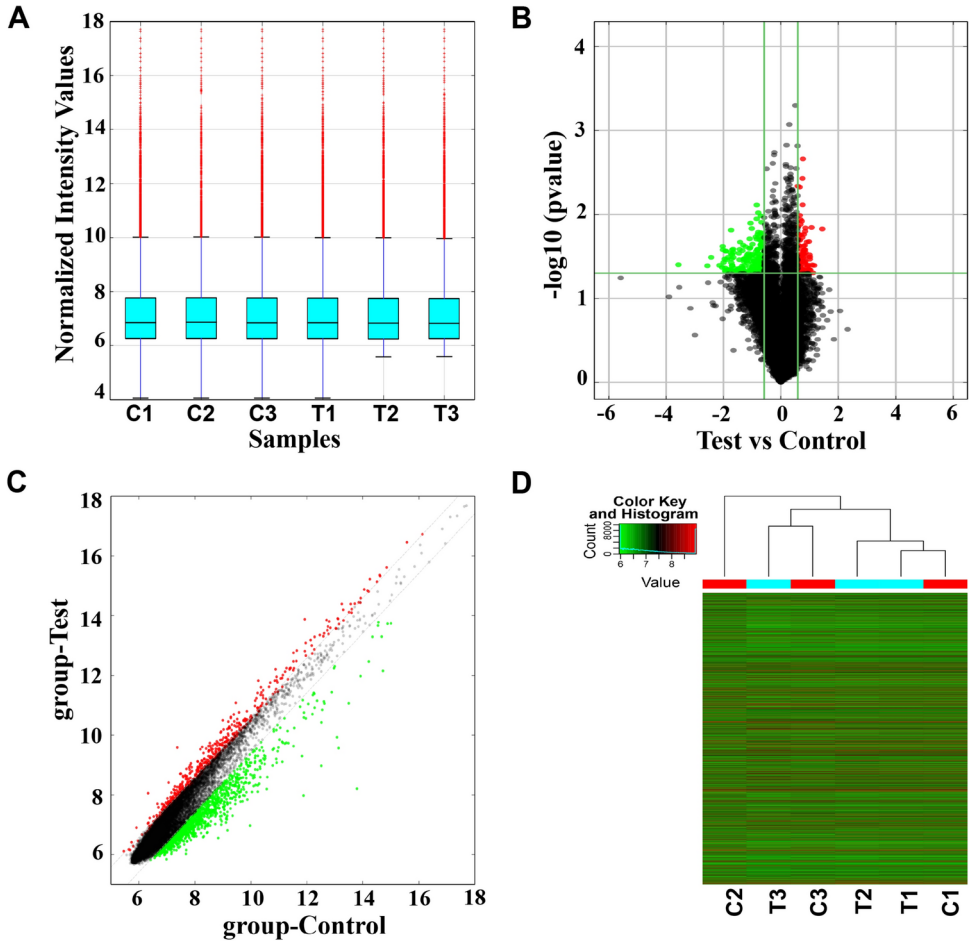

Fig. 2. CircRNAs that are differentially expressed in the liver tissue of CIH mice. (**A**) The box plot illustrates the normalization of circRNA expression intensity values through log transformation, with the red data points indicating outliers. (**B**) The vertical lines indicate a 1.5-fold change in either direction, while the horizontal line illustrates a p-value of 0.05. The red points on the plot signify circRNAs with statistically significant differential expression. (**C**) Scatter plot of differentially expressed circRNAs between CIH and control groups. (**D**) A hierarchical clustering analysis of DECs is presented. C: Control group; T: CIH group.

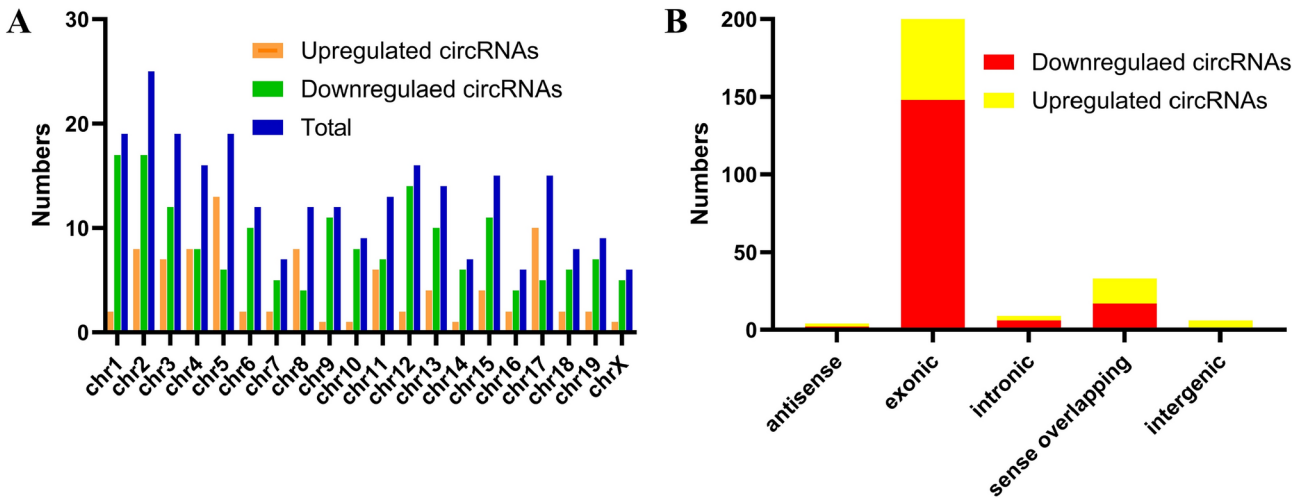

Fig. 3. Features of DECs in the CIH group. (**A**) A clustering diagram shows how dysregulated circRNAs are distributed across various chromosomes. (**B**) A categorization of the markedly changed circRNAs in the CIH group is provided.

sense-overlapping, 3 are intronic, 6 are intergenic, and 2 are antisense. Conversely, among the downregulated circRNAs, 148 are exon-containing, 17 are sense-overlapping, 6 are intronic, and 2 are antisense (Fig. 3B).

Validation of eight selected dysregulated circRNA expressions

To improve the dependability of the outcomes from microarray analysis, qRT-PCR was employed to analyze eight circRNAs, selected based on their p-values, fold changes, lengths, and initial signal intensities. This analysis involved eight circRNAs, of which four were upregulated (mmu_circRNA_36790, 37101, 35781, and 36551) and four were downregulated (mmu_circRNA_44178, 38959, 38398, and 25178). The data confirm that the qRT-PCR results correspond to the outcomes of the microarray analysis (Fig. 4). β-actin served as the internal control.

In-depth analysis of circRNA-miRNA interactions

In order to delve deeper into the eight confirmed circRNAs, including mmu_circRNA_36790, 37101, 35781, 36551, 44178, 38959, 38398, and 25178, we predicted their corresponding target miRNAs using MiRanda and TargetScan. Figure 5 presents the top five identified miRNAs, while the top five predicted interaction sites for mmu_circRNA_35781 are mmu-miR-103-3p, 218-1-3p, 496b, 7020-5p, and 7647-3p (Fig. 6).

Construction of the ceRNA interaction network

A single circRNA can interact with multiple miRNAs and multiple mRNAs, and vice versa. To gain a deeper understanding of the biochemical mechanisms underlying the DECs, we selected three circRNAs (mmu_circRNA_35781, 38959, and 38398) to create a comprehensive regulatory map integrating circRNA-miRNA-mRNA. This ceRNA network comprised 37 miRNAs, 70 messenger RNAs (mRNAs), and 3 circRNAs. Analyzing this network provides critical insights into the molecular mechanisms by which circRNAs contribute to OSA-induced liver damage, suggesting that circRNAs may function as ceRNAs (Fig. 7).

Investigation of GO and KEGG pathways

To delve deeper into the functional roles of the target genes of circRNAs, we performed GO and KEGG analyses on the genes previously validated. As shown in Fig. 8, DECs and mRNAs showed significant enrichment in GO terms related to BP, CC, and MF (Fig. 8A,B). Notably, the most prominent enrichment among both upregulated and downregulated DECs was observed in the "Intracellular anatomical structure" category. This analysis highlighted the significant roles of these target genes in processes such as ion binding, anion binding, intracellular organelle function, organelle lumen dynamics, nitrogen compound metabolism, and cellular component organization. In addition, KEGG pathway analysis demonstrated that the target genes were predominantly enriched in pathways related to chemical carcinogenesis, alcoholic liver disease, the NOD-like receptor pathway, fatty acid degradation, the viral life cycle, tryptophan metabolism, and the degradation of valine, leucine, and isoleucine. Among these, the majority of the downregulated DECs were associated with chemical carcinogenesis, while the upregulated circRNAs were associated with the NOD-like receptor pathway (Fig. 9A,B).

Discussion

In our research, we conducted a detailed exploration of circRNA expression profiles in liver impairment using a CIH-induced mouse model. Utilizing bioinformatics analysis, we pinpointed several essential circular RNAs participated in the biological mechanisms initiated by liver injury resulting from OSA. This research not only expands our insight into the fundamental mechanisms of liver damage linked to OSA but also lays the groundwork for innovative clinical applications. This underscores the potential for circRNAs to revolutionize

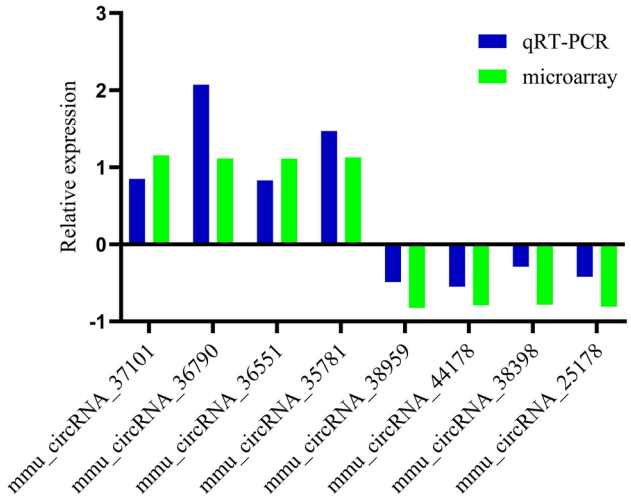

Fig. 4. Outcomes of the qRT-PCR validation for the circRNAs that were selected.

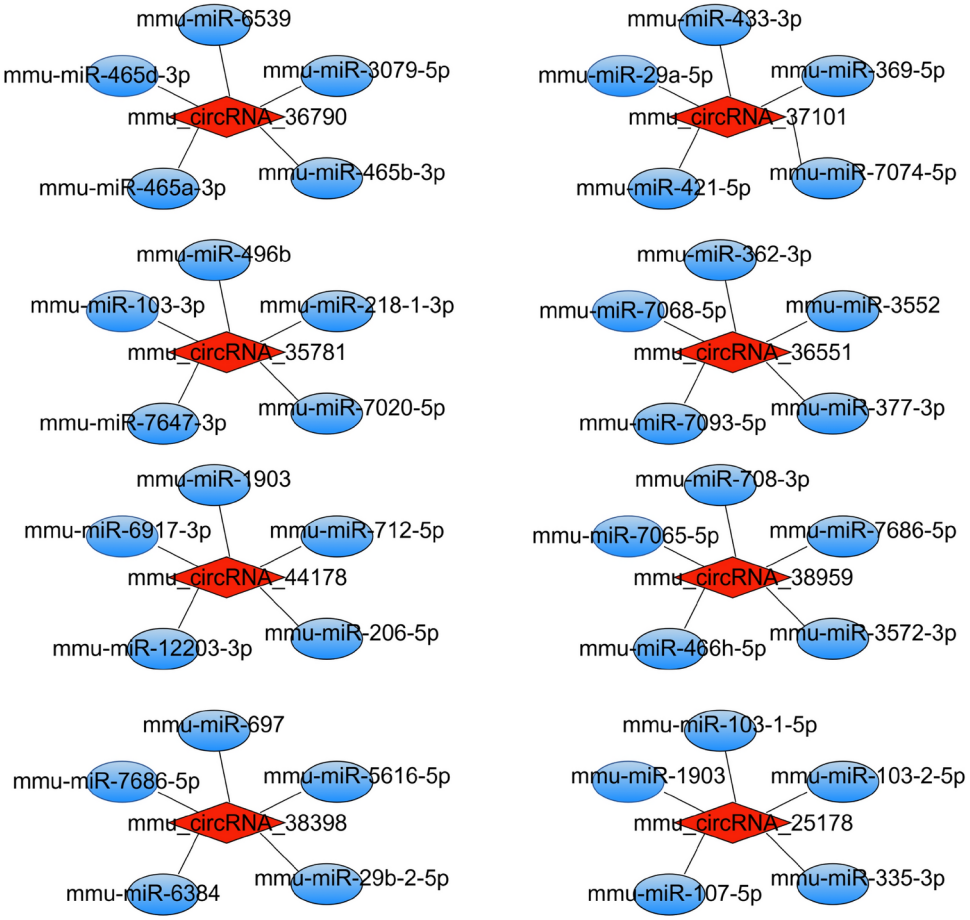

Fig. 5. The top five anticipated targets from 8 verified circRNAs.

the clinical management of such conditions, offering a promising direction for future research and treatment development.

Research has shown that OSA is strongly associated with various systemic diseases, particularly cardiovascular diseases, metabolic disorders, and respiratory diseases. Although the specific mechanisms by which OSA causes liver damage are not yet fully understood, research indicates that CIH leads to tissue hypoxia, resulting in oxidative stress, mitochondrial dysfunction, and inflammatory responses[18], alongside excessive activation of the sympathetic nervous system[19]. These physiological changes may not only trigger hepatic steatosis but also accelerate the progression of fibrosis. This suggests that CIH has profound effects on the function of multiple organs, particularly in exacerbating liver disease through oxidative stress and inflammation. Understanding these mechanisms will aid in the clinical treatment and prevention of liver diseases triggered by OSA.

CircRNAs are a class of RNA with a unique circular structure produced through a reverse splicing process[20]. This structure confers high stability, conservation, and tissue-specific expression, allowing circRNAs to play significant roles in various biological processes[21,22]. CircRNAs have been confirmed to be strongly related to cardiovascular diseases[23], neurological disorders[24], diabetes[25] and cancer[26] indicating their essential function in regulating the occurrence, progression, and treatment of these diseases. This study used circRNA microarray technology to analyze the circRNA expression patterns in CIH-induced mouse liver damage. Our results revealed significant variations in circRNA expression profiles between the CIH and control groups, with 173 circRNAs downregulated and 86 circRNAs upregulated. We further analyzed the types and chromosomal locations of these DECs. Additionally, we randomly selected eight circRNAs with abnormal expression for validation via qRT-PCR, confirming the significant impact of circRNAs on the onset and progression of liver damage induced by OSA. This rapid advancement in circRNA research might pave the way for developing cutting-edge strategies to diagnose and treat liver injuries caused by OSA.

Many circRNAs are instrumental in key biological activities by acting as miRNA or protein absorbers ('sponges'), influencing protein activity or engaging in self-translation. Although the functional significance and mechanisms of circRNAs are still being actively explored, they are believed to modulate host genes transcription and sequester miRNAs and RNA-binding proteins[27,28]. This further influences the expression of target genes. For instance, previous research has established that hsa_circ_0110102, acting as an inhibitor for miR-580-5p, inhibits the secretion of CCL2 into the tumor microenvironment by suppressing the expression of PPARα in hepatocellular carcinoma cells. This mechanism subsequently leads to the inhibition of pro-inflammatory cytokine release in macrophages through the modulation of the COX-2/PGE2 pathway[29]. In our study, we

Fig. 6. Expected binding sites for mmu_circRNA_35781.

established a ceRNA interaction network to elucidate how circRNA functions in the liver damage model induced by CIH in mice. Our study revealed that three confirmed circRNAs (mmu_circRNA_35781, 38959, and 38398) actively target 37 miRNAs. Notably, mmu_circRNA_35781 was significantly upregulated, suggesting its potential involvement in CIH-induced liver damage by inhibiting miRNA functions. Our analysis of circRNA and miRNA pointed to the likely target miRNAs of mmu_circRNA_35781, which include mmu-miR-7020-5p, 496b, 218-1-3p, 7647-3p, and 103-3p. Furthermore, the ceRNA network identified new associations between dysregulated circular RNAs and 70 mRNAs. Importantly, the network provides robust evidence supporting the

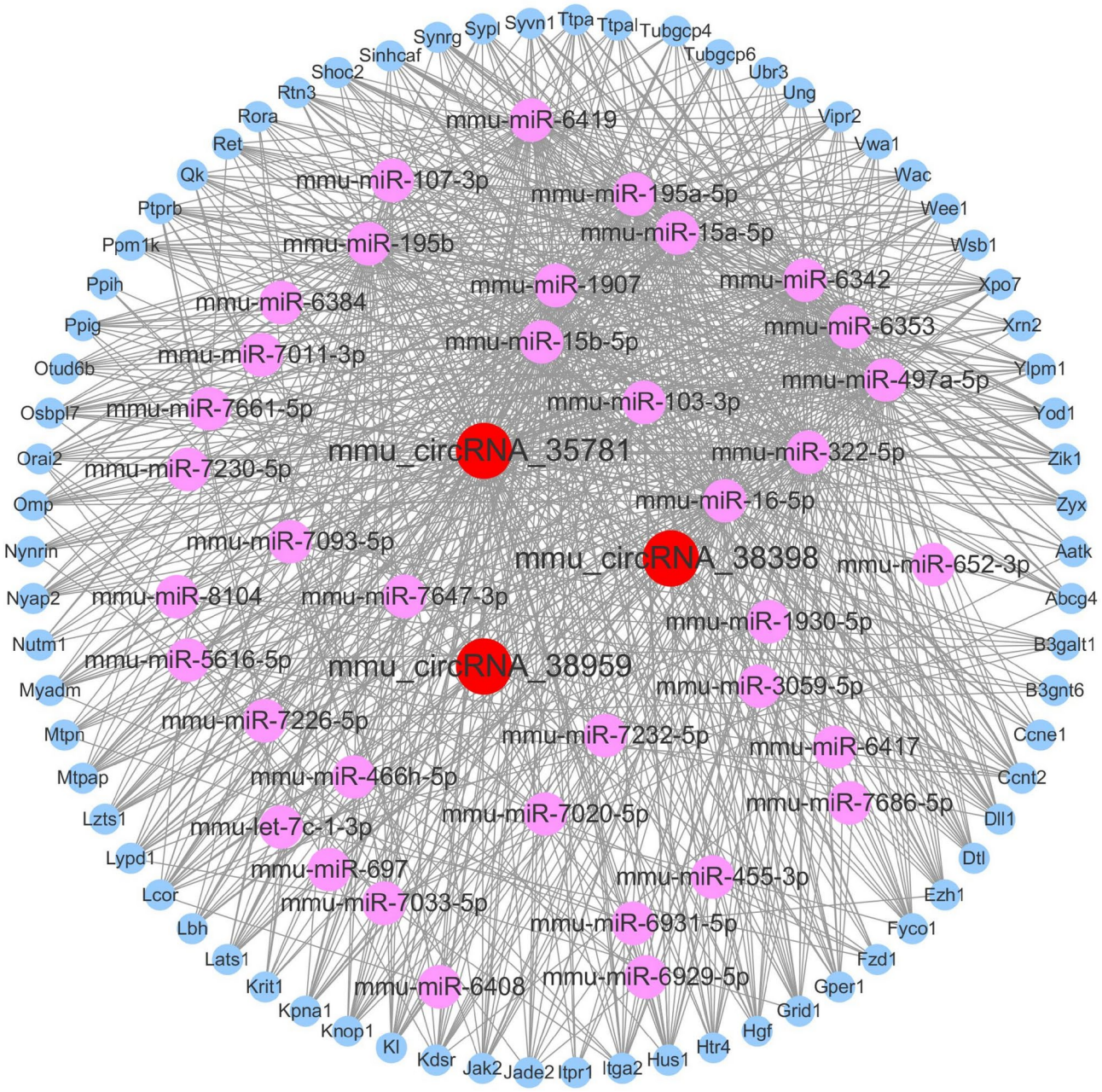

Fig. 7. The ceRNA Network Construction. The regulatory system comprises 37 miRNAs, 3 circRNAs, and 70 mRNAs. The blue, purple, and red nodes represent mRNA, miRNA, and circRNA, respectively.

significant role of circRNAs in the pathogenesis of liver damage caused by OSA through the indirect modulation of specific mRNAs.

To better understand how target genes contribute to the ceRNA network, we also conducted GO and KEGG analyses. The molecular function analysis highlighted processes such as ion binding and anion binding. The assessment of cellular components revealed that the dysregulated circRNA target genes are mainly associated with intracellular anatomical structures, organelles, and cellular anatomical entities. Analysis of biological processes showed that the target genes are mainly related to cellular activities and metabolic processes. By conducting KEGG analysis, we identified multiple key pathways associated with the NOD-like receptor pathway (NLR), chemical carcinogenesis-reactive oxygen species, and tryptophan metabolism. Multiple studies indicate that the NLR plays a pivotal role in immune responses by triggering inflammatory processes[30–32]. Moreover, the activation of the NLR pathway is involved in organ damage induced by CIH[33,34]. Therefore, we believe that the NLR pathway plays a significant role in CIH-induced liver injury. In the context of liver damage, the activation of this pathway likely exacerbates oxidative stress and inflammation, further contributing to liver dysfunction. However, our study did not delve into the intricate mechanisms underlying the identified DECs, leaving a significant gap in understanding their roles. Future studies are necessary to explore the biological functions and

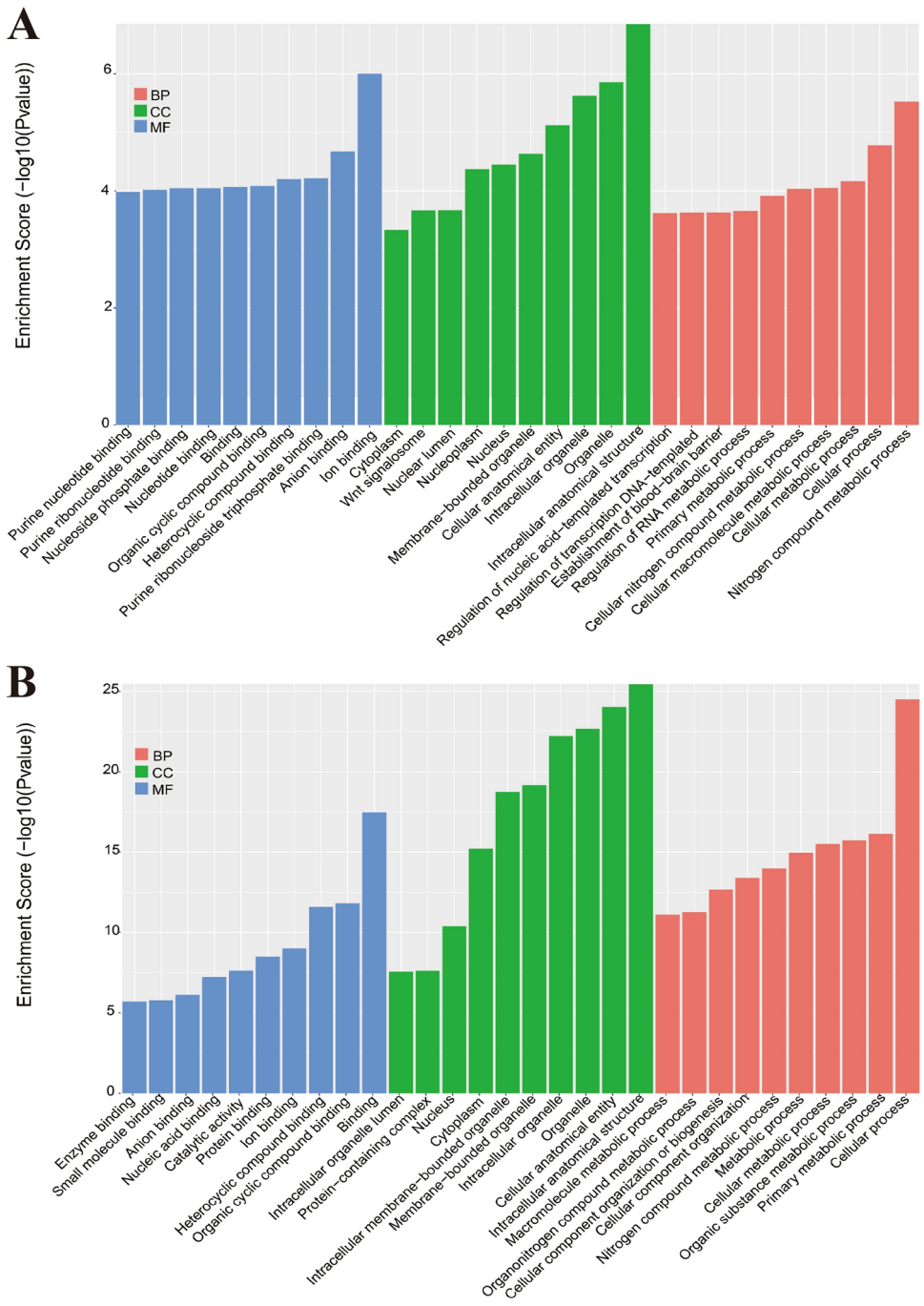

Fig. 8. Go analysis of changed circRNAs. (**A**) GO enrichment analysis for upregulated. (**B**) GO enrichment analysis for downregulated.

pathways associated with these circRNAs to comprehensively elucidate their contributions in the context of liver injury.

Although we systematically analyzed the circRNA expression profiles in CIH-induced mouse liver damage, several limitations of our study warrant attention. Firstly, the scope of this research is somewhat limited by the finite sample size, highlighting the importance of larger samples in future work. Secondly, the potential molecular regulatory mechanisms and functions of circRNA in OSA-induced liver damage require further investigation. Thirdly, the diagnostic effectiveness of circRNA levels should be analyzed in different, more accessible, and less invasive samples, such as exosomes and hair samples. This could enhance clinical feasibility as they might serve as diagnostic biomarkers for the progression of liver injury related to obstructive sleep apnea. Fourthly, the exclusive use of male APOE mice in our study restricts the generalizability of the results to other biological sexes. Incorporating female mice in future research would improve the reliability of the findings and enhance their relevance to a broader population. Fifthly, one potential concern is whether APOE deficiency

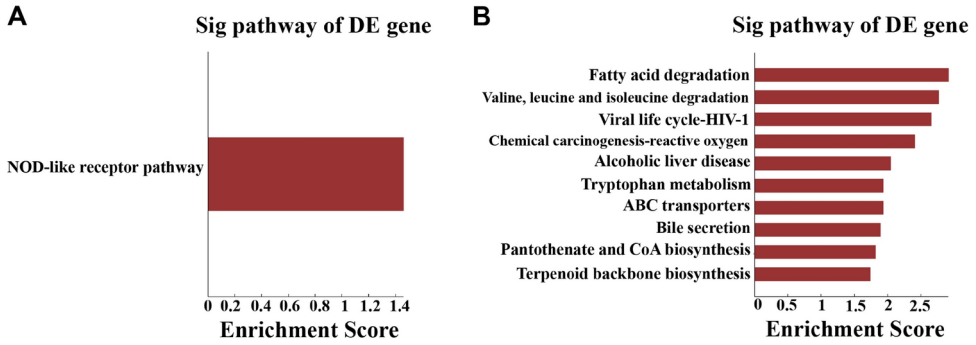

Fig. 9. KEGG analysis of changed circRNAs. (**A**) KEGG analysis for upregulated circRNAs. (**B**) KEGG analysis for downregulated circRNAs.

itself might contribute to hepatic injury, thereby confounding the observed effects of CIH. However, APOE mice were specifically chosen due to their well-established role in studying metabolic and hepatic disorders. Importantly, both the CIH and control groups in our study were APOE-deficient, ensuring that any observed differences in liver injury were primarily attributable to CIH exposure rather than APOE deficiency itself. Nonetheless, to further validate our findings, future studies using wild-type mice or alternative models could provide additional insights into the role of circRNAs in OSA-induced liver damage. Sixthly, our study focused on performing circRNA microarray analysis on liver tissues following model induction, accompanied by a series of bioinformatics analyses and predictions, including the circRNA-miRNA-mRNA ceRNA network prediction. However, at this stage, we have not yet conducted luciferase targeting assays to experimentally validate the predicted interactions. Lastly, our animal model differs significantly from the human OSA model, and our study was conducted solely on the animal model.

Conclusions

In conclusion, this study evident that circRNAs exhibit a differential expression profile in a murine model of liver injury induced by OSA. This suggests that circRNAs could be implicated in the pathogenesis of liver damage caused by CIH, a hallmark of OSA. The potential therapeutic implications of modulating circRNAs to treat liver diseases associated with OSA are thus highlighted by these discoveries. The comprehensive analysis of these results sheds light on the possibility of targeting circRNAs for therapeutic interventions in OSA-related liver disorders. However, further research is warranted to elucidate the precise role and underlying mechanisms of circRNAs in liver injury induced by OSA.

Data availability

The microarray data generated and analyzed in this study is publicly available through the GEO database under accession number GSE282153. The dataset can be accessed at https://www.ncbi.nlm.nih.gov/geo/query/acc.cgi?acc=GSE282153 using the access token azuragowlxctbmf.

Received: 12 January 2025; Accepted: 21 April 2025
Published online: 04 May 2025

References

1. Gleeson, M. & McNicholas, W. T. Bidirectional relationships of comorbidity with obstructive sleep apnoea. *Eur. Respir. Rev.* https://doi.org/10.1183/16000617.0256-2021 (2022).
2. Yeghiazarians, Y. et al. Obstructive sleep apnea and cardiovascular disease: A scientific statement from the American Heart Association. *Circulation* **144**, e56–e67. https://doi.org/10.1161/cir.0000000000000988 (2021).
3. Redline, S., Azarbarzin, A. & Peker, Y. Obstructive sleep apnoea heterogeneity and cardiovascular disease. *Nat. Rev. Cardiol.* **20**, 560–573. https://doi.org/10.1038/s41569-023-00846-6 (2023).
4. Martinot, J. B., Le-Dong, N. N., Malhotra, A. & Pépin, J. L. Respiratory effort during sleep and prevalent hypertension in obstructive sleep apnoea. *Eur. Respir. J.* https://doi.org/10.1183/13993003.01486-2022 (2023).
5. Liu, T. et al. Effect of obstructive sleep apnoea on coronary collateral vessel development in patients with ST-segment elevation myocardial infarction. *Respirology* **27**, 653–660. https://doi.org/10.1111/resp.14277 (2022).
6 Javaheri, S. & Javaheri, S. Obstructive sleep apnea in heart failure: Current knowledge and future directions. *J. Clin. Med.* https://doi.org/10.3390/jcm11123458 (2022).
7. Zhang, L. et al. Obstructive sleep apnea and liver injury in severely obese patients with nonalcoholic fatty liver disease. *Sleep Breath* **24**, 1515–1521. https://doi.org/10.1007/s11325-020-02018-z (2020).
8. Preshy, A. & Brown, J. A bidirectional association between obstructive sleep apnea and metabolic-associated fatty liver disease. *Endocrinol. Metab. Clin. N. Am.* **52**, 509–520. https://doi.org/10.1016/j.ecl.2023.01.006 (2023).
9. Patop, I. L., Wüst, S. & Kadener, S. Past, present, and future of circRNAs. *Embo J.* **38**, e100836. https://doi.org/10.15252/embj.2018100836 (2019).
10. Kristensen, L. S. et al. The biogenesis, biology and characterization of circular RNAs. *Nat. Rev. Genet.* **20**, 675–691. https://doi.org/10.1038/s41576-019-0158-7 (2019).
11. Huang, X. Y. et al. Exosomal circRNA-100338 promotes hepatocellular carcinoma metastasis via enhancing invasiveness and angiogenesis. *J. Exp. Clin. Cancer Res.* **39**, 20. https://doi.org/10.1186/s13046-020-1529-9 (2020).

12. Hansen, T. B. et al. Natural RNA circles function as efficient microRNA sponges. *Nature* **495**, 384–388. https://doi.org/10.1038/nature11993 (2013).
13. Zeng, P., Cai, X., Yu, X. & Gong, L. Markers of insulin resistance associated with non-alcoholic fatty liver disease in non-diabetic population. *Sci. Rep.* **13**, 20470. https://doi.org/10.1038/s41598-023-47269-4 (2023).
14. Huang, G. et al. CircRNA hsa_circRNA_104348 promotes hepatocellular carcinoma progression through modulating miR-187–3p/RTKN2 axis and activating Wnt/β-catenin pathway. *Cell Death Dis.* **11**, 1065. https://doi.org/10.1038/s41419-020-03276-1 (2020).
15. Kanehisa, M. Toward understanding the origin and evolution of cellular organisms. *Protein Sci.* **28**, 1947–1951. https://doi.org/10.1002/pro.3715 (2019).
16. Kanehisa, M. & Goto, S. KEGG: Kyoto encyclopedia of genes and genomes. *Nucleic Acids Res.* **28**, 27–30. https://doi.org/10.1093/nar/28.1.27 (2000).
17. Kanehisa, M., Furumichi, M., Sato, Y., Kawashima, M. & Ishiguro-Watanabe, M. KEGG for taxonomy-based analysis of pathways and genomes. *Nucleic Acids Res.* **51**, D587–D592. https://doi.org/10.1093/nar/gkac963 (2023).
18. Fernandes, J. L. et al. Chronic intermittent hypoxia-induced dysmetabolism is associated with hepatic oxidative stress. *Mitochondrial Dysfunct. Inflamm. Antioxid.* https://doi.org/10.3390/antiox12111910 (2023).
19. Mesarwi, O. A., Loomba, R. & Malhotra, A. Obstructive sleep apnea, hypoxia, and nonalcoholic fatty liver disease. *Am. J. Respir. Crit. Care Med.* **199**, 830–841. https://doi.org/10.1164/rccm.201806-1109TR (2019).
20. Yang, Q., Li, F., He, A. T. & Yang, B. B. Circular RNAs: Expression, localization, and therapeutic potentials. *Mol. Ther.* **29**, 1683–1702. https://doi.org/10.1016/j.ymthe.2021.01.018 (2021).
21. Nemeth, K., Bayraktar, R., Ferracin, M. & Calin, G. A. Non-coding RNAs in disease: from mechanisms to therapeutics. *Nat. Rev. Genet.* **25**, 211–232. https://doi.org/10.1038/s41576-023-00662-1 (2024).
22. Zhang, Y., Zhan, L., Jiang, X. & Tang, X. Comprehensive review for non-coding RNAs: From mechanisms to therapeutic applications. *Biochem. Pharmacol.* **224**, 116218. https://doi.org/10.1016/j.bcp.2024.116218 (2024).
23. Mei, X. & Chen, S. Y. Circular RNAs in cardiovascular diseases. *Pharmacol. Ther.* **232**, 107991. https://doi.org/10.1016/j.pharmthera.2021.107991 (2022).
24. Wu, D. P. et al. Circular RNAs: Emerging players in brain aging and neurodegenerative diseases. *J. Pathol.* **259**, 1–9. https://doi.org/10.1002/path.6021 (2023).
25. Fan, W., Pang, H., Xie, Z., Huang, G. & Zhou, Z. Circular RNAs in diabetes mellitus and its complications. *Front. Endocrinol.* **13**, 885650. https://doi.org/10.3389/fendo.2022.885650 (2022).
26. He, Z. & Zhu, Q. Circular RNAs: Emerging roles and new insights in human cancers. *Biomed. Pharmacother.* **165**, 115217. https://doi.org/10.1016/j.biopha.2023.115217 (2023).
27. Mehta, S. L., Dempsey, R. J. & Vemuganti, R. Role of circular RNAs in brain development and CNS diseases. *Prog. Neurobiol.* **186**, 101746. https://doi.org/10.1016/j.pneurobio.2020.101746 (2020).
28. Kristensen, L. S. et al. The biogenesis, biology and characterization of circular RNAs. *Nat. Rev. Genet.* **20**, 675–691. https://doi.org/10.1038/s41576-019-0158-7 (2019).
29. Wang, X. et al. CircRNA hsa_circ_0110102 inhibited macrophage activation and hepatocellular carcinoma progression via miR-580-5p/PPARα/CCL2 pathway. *Aging* **13**, 11969–11987. https://doi.org/10.18632/aging.202900 (2021).
30. Wang, L. & Hauenstein, A. V. The NLRP3 inflammasome: Mechanism of action, role in disease and therapies. *Mol. Asp. Med.* **76**, 100889. https://doi.org/10.1016/j.mam.2020.100889 (2020).
31. Kong, P. et al. Inflammation and atherosclerosis: signaling pathways and therapeutic intervention. *Signal Transduct. Target Ther.* **7**, 131. https://doi.org/10.1038/s41392-022-00955-7 (2022).
32. Jo, E. K., Kim, J. K., Shin, D. M. & Sasakawa, C. Molecular mechanisms regulating NLRP3 inflammasome activation. *Cell Mol. Immunol.* **13**, 148–159. https://doi.org/10.1038/cmi.2015.95 (2016).
33. Wu, X. et al. NLRP3 deficiency protects against intermittent hypoxia-induced neuroinflammation and mitochondrial ROS by promoting the PINK1-parkin pathway of mitophagy in a murine model of sleep apnea. *Front. Immunol.* **12**, 628168. https://doi.org/10.3389/fimmu.2021.628168 (2021).
34. Wu, X., Chang, S. C., Jin, J., Gu, W. & Li, S. NLRP3 inflammasome mediates chronic intermittent hypoxia-induced renal injury implication of the microRNA-155/FOXO3a signaling pathway. *J. Cell Physiol.* **233**, 9404–9415. https://doi.org/10.1002/jcp.26784 (2018).

Author contributions

This article was drafted by Huiting Lai and Yuwei Chen. The conceptualization and design of the experiments were developed by Qingshi Chen and Dexin Liu. Huiting Lai, Yuwei Chen, and Zhuli Peng conducted the experiments and performed data analysis and validation. Dexin Liu and Siying Wu analyzed the data and prepared the figures and/or tables. The final manuscript was reviewed and approved by all authors.

Funding

This work was supported by the Joint Funds for the innovation of science and Technology, Fujian province (Grant number: 2021Y9027), Fujian Provincial Natural Science Foundation of China (Grant number: 2024J01662), Fujian Medical University Student Innovation and Entrepreneurship Training Program Funding Project (Grant Numbers: C2024051 and JC2023180), Quanzhou Science and Technology Projects (Grant number: 2022C038R), Natural Science Foundation of Fujian Province (Grant Number: 2023J01719), and Medical Innovation Project of Fujian Provincial Health Science and Technology Program (Grant Number: 2023CXA034).

Competing interests

The authors declare no competing interests.

Additional information

Supplementary Information The online version contains supplementary material available at https://doi.org/10.1038/s41598-025-99612-6.

Correspondence and requests for materials should be addressed to Q.C. or D.L.